Title

Epidural spinal stimulation is associated with changes in surviving axons and associated glial cells after spinal cord injury in rodents

Author

DePetro, Kyleigh Alexis

Publication Date

2017

Peer reviewed|Thesis/dissertation

UNIVERSITY OF CALIFORNIA

Los Angeles

Epidural spinal stimulation is associated with changes in surviving axons and associated glial cells after spinal cord injury in rodents

A thesis submitted in partial satisfaction

of the requirements for the degree of Master of Science

in Physiological Science

by

Kyleigh Alexis DePetro

2017

ABSTRACT OF THE THESIS

Epidural spinal stimulation is associated with changes in surviving axons and associated glial cells after spinal cord injury in rodents

by

Kyleigh Alexis DePetro

Master of Science in Physiological Science

University of California, Los Angeles, 2017

Professor Victor R. Edgerton, Chair

We previously demonstrated that epidural spinal stimulation (ES) and transcutaneous stimulation combined with step training can restore voluntary motor control in humans with chronic, motor-complete spinal cord injuries in at least 24 hours. The purpose of this study was to determine the underlying pathways involved. We hypothesized that chronic ES can provide motor improvements that persist in the absence of stimulation and that both surviving axons and their associated glial cells play important roles in ES-facilitated recovery. Our kinematic data suggested that chronic ES is associated with persistent motor recovery when ES is off. Our histological analysis demonstrated that the node of Ranvier, oligodendrocytes, astrocytic process extension, and apoptosis play important roles in mediating axonal integrity associated with functional motor improvement with ES in rats.

The thesis of Kyleigh Alexis DePetro is approved.

Cristina A. Ghiani

Christopher S. Colwell

Barnett Schlinger

Victor R. Edgerton, Committee Chair

University of California, Los Angeles

2017

TABLE OF CONTENTS

LIST OF FIGURES

ACKNOWLEDGEMENTS

I would like to express my gratitude to the following individuals:

Professor V. Reggie Edgerton, Ph.D., Committee Chair, who welcomed me into his laboratory and provided continuous guidance and support while inspiring me to think critically about research.

Committee members: Professor Cristina A. Ghiani, Ph.D., Professor Christopher S. Colwell, Ph.D., and Professor Barnett Schlinger, Ph.D., for their experimental design insight, data analysis feedback, and editorial efforts in preparing this thesis.

Professor Niranjala Tillakaratne, Ph.D., for her kind and compassionate mentorship over the years.

Dr. Hui Zhong, M.D., for performing all animal surgeries and advisement in animal care.

Professor Cristina A. Ghiani, Ph.D., for guiding me through confocal microscopy and providing insight on glial cell involvement in motor recovery.

Czarina Juan-Sing, B.S., for tremendous efforts in animal care, immunostaining, and quantification.

Sharon Zdunowski, B.S., for assisting in kinematic data acquisition and analysis.

Emilie Liu, for assistance in quantification of spinal lesion cavity areas.

Bau Pham, Ph.D. candidate, for assisting in microscopy and immunostaining troubleshooting.

Dr. Kazu Kobayakawa, M.D., Ph.D., for his guidance on tissue processing, quantification, and mechanistic insight.

Dustin Sandoval, for all of his love, patience, and support throughout my academic career.

Jeff DePetro, Amber DePetro, Julie DePetro, and the rest of my family for their inspiration and encouragement.

Dana & Albert R. Broccoli Charitable Foundation, for funding this thesis research.

Introduction

Spinal cord injury overview

Many spinal cord injuries (SCI) are anatomically incomplete, yet result in complete loss of motor function. Often, it is presumed that a spinal cord lesion results in permanent loss of control, without the prospect of significant motor improvement. In fact, by two years post-SCI, the individual is not expected to make significant improvements in recovery throughout the time course of their life. This prognosis has several important implications not only for their physical abilities, but their mental health, relationships, and life goals- The rate of depression and other comorbid psychopathology is increased in the SCI population and has been associated with reduced life expectancy (Craig et al., 2008). This makes the challenge of motor function rehabilitation a critical issue for increasing the longevity and quality of life of this population.

Approaches to motor recovery post-SCI and the use of epidural stimulation to restore voluntary movement

Efforts to regain motor function post-SCI have traditionally involved the use of various stem cells, bioscaffolds, neurotrophic factors and Nogo-A antibodies to promote neuroregeneration of lesioned spinal axons through the glial scar formed by the lesion (Liebscher et al., 2005). The objective has been to make functional connections able to sufficiently promote neural communication between the brain and spinal networks caudal to the lesion for both planning and execution of voluntary movement. While this approach has shown some promise, and theoretically has potential, the magnitude of the challenges is enormous. Some important uncertainties include: Selection of the most

effective cell type, dosage, administration frequency, host receptivity, and use of the most appropriate implantable biomaterials are among some of the intricate variables that need to be considered for supporting neuroregeneration that both is ethically sound and practical (Pêgo et al., 2012). Given recent demonstrations of motor improvement within even a single session of transcutaneous spinal neuromodulation in chronic, motor-complete paralysis, it appears that the basic biology of the spinal lesion has repairable features not previously recognized. Thus, we asked, whether some spinal axons and their associated glial cells, which anatomically survive the initial injury, can be therapeutic targets for ES-facilitated motor recovery post-SCI.

We hypothesize that at least some cells and axons survive the initial injury and are capable of maintaining some potential for forming functional connections with interneurons and motor pools below the lesion. Our lab recently demonstrated that humans with chronic, motor- and/or sensory- complete SCI can regain on-command voluntary motor function of the lower limbs within a single session of transcutaneous spinal stimulation (ES) (Angeli et al., 2014; Harkema et al., 2011). This unexpected recovery implies that “silenced” or dormant spinal axons that contribute to the chronic motor- or sensory-complete phenotype may be “awakened” or modulated to a critical level that allows neural conduction between the brain and peripheral muscles for movement. While we have demonstrated recovery in nine individuals, the molecular mechanisms associated with this regain of motor function are not well understood (Angeli et al., 2014; Gerasimenko et al., 2015; Harkema et al., 2011). Understanding how ES facilitates motor recovery post-SCI is critical and it seems very likely that the advancement of rehabilitation

will include methods of optimization of stimulation parameters. ES is already FDA-approved for treatment of chronic neuropathological pain in humans. However, safety evaluations on the efficacy of chronic ES use for motor improvement, are currently being conducted by our lab and collaborators. Those studies may also provide a better understanding of how some components of the spinal circuitry can survive a SCI, yet display the level of neuroplasticity that has been reported to improve motor control in the post-injury state. These new findings open an entire realm of possibilities with therapeutic potential.

Intact spinal axon node of Ranvier and associated glial cells as targets for ES-facilitated motor recovery

The current study focuses on whether and how ES may modulate both the neural axons that remain intact post-injury (axons contralateral to a lesion or in and around a contusive SCI) and their associated glial cells. We believe the time for recovery of motor function associated with ES is too short to be attributed to functional axonal growth across the lesion. Both neuron axons and glial cells become disrupted post-SCI and result in loss of conduction and motor output (Arvanian et al., 2009; Hununyan et al., 2011; Wang et al., 2017). Still, it is important to realize that the involved pathways by which ES facilitates motor recovery are likely to be multifactorial and complex, given the significant interneuronal connectivity within the nervous system that has been observed.

Nonetheless, previous rodent studies have demonstrated that there exist axons that survive the initial injury, but are converted to a “dormant” state in the weeks post-injury

and this dormancy is associated with reduced motor function (Arvanian et al., 2009; Hununyan et al., 2010). These axons develop reduced conduction speed, increased latency, and lower volley amplitude associated with dispersed voltage-gated sodium channel isoform 1.6 (Nav1.6) beginning 1-2 weeks post-injury and persisting for at least 16 weeks. Because Nav1.6 is the predominant ion channel at the node of Ranvier in mature axons, normal channel clustering at the node is necessary for conduction of the action potential and motor function (Huxley and Stämpfli, 1949; Susuki et al., 2013). The axo-glial junction and molecules such as glia-derived extracellular matrix (ECM), NF186, and NF155 (among others) mediate the glial process contact at the axolemma node of Ranvier to maintain ion channel clustering and nodal morphological integrity (Huxley and Stämpfli, 1949; Taylor et al., 2017; Waxman et al., 1994). Further, loss of these components at the node of Ranvier, by ablation or mutation, reflect a nodal pathology that could account for a loss of conduction and axonal degeneration nonconductive to motor recovery (Taylor et al., 2017). Thus, we hypothesize that ES-facilitated recovery may be associated with effects or modulation of glial cells at the node of Ranvier and maintenance or preservation of the nodal channel clustering integrity.

The relationship between oligodendrocytes, astrocytes, and associated neuronal axons in ES-mediated motor recovery

Oligodendrocytes are the only myelinating glial cells of the central nervous system (CNS) (Leferink and Heine, 2017). They are important for saltatory conduction as they extend the myelin sheaths, creating the insulated fatty internodal regions of axons. CNS insult, regardless of neuronal cell body destruction, can trigger axonal degeneration and/or

compromise myelin integrity involving the net loss of mature myelinating oligodendrocytes. This occurs in demyelinating disorders, such as SCI, and can be a devastating downstream effect of the initial insult to the CNS (Leferink and Heine, 2017). While this association highlights the potential importance of the enwrapping oligodendrocyte in maintaining axon integrity, it also identifies the system as a candidate therapeutic target post-SCI. If one cell can be modulated by a given therapy, such as ES, perhaps this can ameliorate pathology in associated cells. This idea is supported by a recent study that shows optogenetic stimulation of the mouse premotor cortex is associated with functional oligodendrogenesis, enhanced myelination, and improved limb swing speed in the weeks post-SCI (Gibson et al., 2014). This demonstrates the need for axonal activation to modulate oligodendrocyte cell fate, proliferation, and downstream function.

Because human studies have demonstrated the ability to regain motor control after the use of at least one to multiple ES sessions, it seems possible that ES-mediated recovery modulates oligodendrocyte differentiation, proliferation, and/or functional myelination through activation of axons proximal to the stimulation site (Angeli et al., 2014; Gibson et al., 2014; Harkema et al., 2011). Thus, ES may affect oligodendrocytes associated with axons that survive the initial SCI, but display demyelinating and other pathological properties associated with motor dysfunction. This idea is supported by the complex, dynamic intercommunication between associated axons and glial cells (Domingues et al., 2016; Gibson et al., 2014). However, if oligodendrocyte population changes are associated with the use of ES, it is likely that other glial cells are also involved in this

recovery pathway given the well-established inter-glial communication nested into the CNS network (Sofroniew and Vinters, 2010; Nedergaard et al., 2003; Halassa et al., 2007; Charles et al., 1991).

Astrocytes, highly branched glial cells that comprise grey matter (protoplasmic astrocytes) and white matter (fibrous astrocytes) are densely scattered throughout the CNS and play a major role in CNS function (Sofroniew and Vinters, 2010). Their numerous processes contact blood vessels, the node of Ranvier, neuronal synapses, and other astrocytes (Nedergaard et al., 2003; Halassa et al., 2007; Sofroniew and Vinters, 2010). Importantly, astrocytes contain functional sodium and potassium channels and respond to axonal and external stimulation (Charles et al., 1991; Halassa et al., 2007). Interestingly, the calcium wave induced in a stimulated astrocyte is transmitted to contacted astrocytes through gap junctions for coordinated astrocytic response (Charles et al., 1991). In the injured state, astrocytes affect oligodendrocyte progenitor cells (OPCs) by changing their differentiation and proliferation abilities and rates, thus having an ultimate effect on the final number and effectiveness of functional mature myelinating oligodendrocytes (Domingues et al., 2016). It is not difficult to imagine that ES of the lumbosacral spinal cord could potentially induce a calcium wave in astrocytes that is transmitted not only locally, but also long-range throughout the axonal networks that survive the initial injury but display functional pathology. Further, it remains possible that this astrocytic response is coordinated with oligodendrocytes that also contact axonal node of Ranvier to mediate axonal integrity and associated ES-facilitated recovery.

Experimental goal and hypotheses

The purpose of this study was to determine underlying pathways involved in ES-mediated motor recovery. We first investigated whether ES can improve motor function- as measured by step height- and then determined if this improvement is time-dependent. That is, can ES improve motor function immediately upon stimulation and/or have a chronic effect on motor function such that motor improvements can persist in the absence of stimulation? We demonstrated that ES may function on two distinct temporal pathways. Specifically, we showed that chronic use of ES (more than 20 sessions of 35-minute duration) provides functional motor improvement that persists for at least 24 hours after the last stimulation session in rats. Next, we investigated the cellular changes involved in this recovery. We hypothesized that changes in the node of Ranvier, oligodendrocytes, astrocyte process extension, the relationship between these two glial cells, and cell apoptosis are associated with the demonstrated motor improvement. Our histological analysis suggested that the node of Ranvier may be a critical component involved in this recovery and that both oligodendrocytes and astrocytes play important roles in mediating axonal integrity associated with functional motor improvement with ES in rats.

Materials and Methods

All experimental procedures were conducted according to National Institute of Health *Guide for the Care and Use of Laboratory Animals* and the University of California, Chancellor's Animal Research Committee (National Research Council, 2011).

Study overview

Adult female Sprague-Dawley rats (n=12) were step/stand trained pre-injury on a treadmill, received right lateral hemisection (HX) at T8-T9 spinal level, and were divided into cohorts such that half received either post-injury step training alone (Tr group, n=6) or step training combined with 95% threshold ES (ES+Tr group, n=6). Animals were step tested pre-injury and at day 29 post-injury and sacrificed the following day. Spinal cord tissue was analyzed for injury severity, node of Ranvier morphology, oligodendrocytes, astrocytic process extension, and apoptosis using immunohistochemistry (Fig. 1).

Surgical procedures and post-surgical animal care

Animal surgeries were conducted under sterile, aseptic conditions with animals deeply anesthetized with isoflurane (1.5-2.5%, veterinary pharmaceutical grade) via oxygen mask. The toe-pinch reflex was assessed prior to and throughout surgery. The surgical bed was heated by a water pump maintained at 37°C to prevent hypothermia. As previously described, in the first surgery, animals were implanted with: 1) electromyography (EMG) electrodes bilaterally into the tibialis anterior (TA) and soleus (SOL) muscles of the hindlimbs, and 2) ES electrodes (anode and cathode) into the L2 and S1 spinal segments (Roy et al., 1991; Shah et al., 2012). In the second surgery, which occurred after pre-injury step training, animals received a right lateral hemisection as previously described (Shah et al., 2012). After all surgeries, animals were placed in a recovery incubator at 37°C until fully awake and then transferred to a fresh cage for individual housing throughout the duration of the study to ensure a cagemate could not remove the implanted stimulation unit. Post-surgery, animals were given buprenorphine

(0.01-0.05 mg/kg body weight, s.c., twice daily, 48 hr. minimum post-op.) and enrofloxacin (2.5 mg/kg body weight, s.c., twice daily, five days post-op.) as analgesia and antibiotic, respectively. Oral enrofloxacin (100 mg/125 mL water, changed every four days for 14 days post-op.) was administered beginning day six post-op. Bladders were expressed two to three times per day for the first week post-injury and as needed thereafter. Animals generally recovered autonomous bladder void function by two weeks post-injury. Animals were kept on a 12-12 hr. light-dark cycle with *ad libitum* access to food and water throughout the duration of the study.

Step training and epidural stimulation protocol

All animals received pre-injury quadrupedal step training without body support assistance for 20 sessions (35 minutes in duration) at speed 21 cm/s on a fully-automated rodent treadmill with no incline. Beginning day five post-injury, all animals received 20 step training sessions (35 minutes in duration). During the first three post-injury training sessions, the treadmill speed was variable between speeds 9 cm/s to 21 cm/s to account for intra-animal stepping ability during acute recovery. The experimenters provided some manual trunk support during the first three training sessions to prevent injury sores to the animals due to flank dragging. Beginning with the fourth post-injury training session, all animals were step trained at speed 21 cm/s for 35 minutes plus one five-minute break for rest and access to water. Manual trunk support was not required beginning with the fourth post-injury training session, although motor deficits were still apparent. Tr rats did not receive ES during their post-injury step training. ES+Tr rats received ES (40 Hz., 200 us duration, rectangular pulse width) of the L2/S1 spinal cord at 95% of the threshold

amplitude required to evoke a palpable muscle contraction of the hindlimb triceps surae muscles (Shah et al., 2012). ES thresholds were determined and adjusted for every ES+Tr animal prior to each step testing and training session. Each animal was step trained at approximately the same time each day.

Locomotor testing

Animals were step tested for locomotor function weekly up to day 29 post-injury using SIMI motion capture software (SIMI Reality Motion Systems, Unterschleissheim, Germany) and camera set-up as previously described and depicted in Fig. 2 (Shah et al., 2012). Retroreflective markers, which allowed for objective limb tracking during kinematic analysis, were placed on the major joints of the hindlimb (Fig. 2). Testing sessions lasted between 15 minutes and one hour, depending on the length of time required to successfully capture 10 consecutive steps on video. Animals were given food as positive enforcement to encourage stepping.

Animals were step tested at approximately the same time of day as their regularly-scheduled step training sessions to control for circadian-mediated changes in locomotor coordination and ability. Each step testing session was conducted approximately 24 hours after each animal's most recent step training session. Tr animals were step tested under one condition only (ES turned off) such that, although they received the device implant, it was not turned on throughout the duration of the study. ES+Tr animals were step tested under two conditions (ES+Tr-Off and ES+Tr-On), but were always step tested with ES off before capturing stepping abilities with ES on. This was done in order to capture any long-

lasting motor effects that persist in the absence of ES for at least 24 hours (since the last training session) prior to capturing acute ES-mediated motor improvement. Fig. 3 depicts the step training and testing protocol for both groups, highlighting the differences and timelines for each.

Kinematic data acquisition

Kinematic data was imported to SIMI motion capture software for tracking analysis. An experimenter manually and semi-automatically identified the retroreflective marker location in space for every frame in a given video (100 frames per second, each video ~1-2 minutes in length). Marker tracking was verified by an independent observer to confirm that the manually designated joint locations were accurate. Three-dimensional coordinates were constructed and processed in MatLab, and exported into a spreadsheet with calculated gait parameters. Data were then uploaded to R Studio as a .csv file and analyzed using the statistical methods described below. Stepping data was composed from a series of 7 to 10 steps per animal, which varied based on the animal's ability and willingness to test in a given testing session. Step height for each individual step was divided by the average pre-injury step height for each animal to yield "normalized" values. This normalization was performed to account for inter-animal differences in natural stepping abilities, which might confound statistical significance for post-injury analysis.

Kinematic analysis of step height

To determine the differences in stepping ability (as measured by normalized step height) by day 29 post-injury, individuals normalized step height values for each step were

averaged per animal and then averaged per group to yield one group average normalized step height. Two-way ANOVA with Tukey's HSD post-hoc test was performed to determine statistical significance and to identify the location of differences, respectively.

Animal sacrifice and tissue processing

Animals were given a lethal injection of sodium pentobarbital (100 mg/kg body weight) intraperitoneally prior to sacrifice via transcardial perfusion with 4% paraformaldehyde (PFA) in cold 0.1M Phosphate Buffered Saline (PBS) at physiological pH. Prior to and throughout the perfusion, animals were confirmed to have a negative toe-pinch reflex. The push-volume (mL) of PFA was determined by calculating double the animal's body weight in grams. Immediately post-procedure, the vertebral column was excised from the carcass, submerged into cold 4% PFA, shielded from light penetrance, and fixed overnight for 18.5 hours at 4°C. The spinal cord was serially-washed in 0.1M PBS (pH=7.32), and stored in 30% sucrose in 0.1M PBS (pH=7.40) for at least one week until the density of the spinal cord was greater than that of the solution to indicate optimal cryoprotection.

The spinal cord was then manually sectioned into blocks of two to four rostral-to-caudal spinal cord segments using a razor blade. 1,1'-Dioctadecyl-3,3,3',3'-Tetramethylindocarbocyanine Perchlorate (DiI) was used to mark the left caudal side of the spinal cord for directionality during the subsequent staining processes. Spinal cord blocks were then embedded in Neg-50™ Frozen Section Medium (Richard-Allan Scientific) upon dry ice and stored at -80°C until cryosectioning.

Injury site spinal cord blocks (T7-T10 spinal level) were cut transversely, at 30-um thickness, on a cryostat (Fig. 4) so that both the contralateral white matter and the injury site (T8-T9 spinal level) were visible in the same tissue section. Sectioned tissue slices were stored in 48-well plates containing 0.1M PBS at physiological pH (one tissue per well) until immunohistochemistry or Nissl staining.

Lesion cavity quantification

Approximately six tissue sections per animal were chosen such that the entire thickness of each spinal cord, from dorsal to ventral, was sampled transversely. This allowed a thorough evaluation of injury site cavities. Tissues were mounted on glass slides, dried overnight at room temperature, and exposed to a series of alcoholic dehydrations and de-fatting procedures for Nissl staining with Cresyl Violet. Nissl-stained tissues were coverslipped using Permount Adhesive and heat-dried in an oven overnight. Using ImageJ, the lesion cavities were outlined with the freehand tool and the area (um^2) within each cavity was determined using the measure function. Cavity areas (um^2) were divided by the total spinal cord area per image (um^2) and multiplied by 100 to yield a lesion percentage of total tissue area for each tissue section per animal (Fig. 5B). Values were then summed per animal and a group average was obtained. Welch's t-test was performed to determine the significance of the difference in means between groups. Experimenters were blinded to animal identity and group to prevent bias in the analysis.

Immunohistochemistry

30-um thick tissue sections were briefly washed in 0.1M PBS and blocked at room temperature for one hour using 2% Normal Donkey Serum (NDS) and 0.3% Triton in 0.1M PBS. Tissues sections were incubated at 4°C overnight, with agitation, in solutions containing 2% NDS, 0.1M PBS, 0.3% Triton, and various combinations of the primary antibodies: Rabbit anti-GFAP polyclonal (1:2000, AB5804, EMD Millipore), goat anti-GSTpi polyclonal (1:800, ab53943, Abcam), rabbit anti-cleaved caspase-3 polyclonal (1:400, AB3623, EMD Millipore), rabbit anti-Nav1.6 polyclonal (1:800, ASC-009, Alomone Labs), and mouse anti-caspr monoclonal (1:300, LS-C123322, LifeSpan BioSciences, Inc.). Following the primary incubations, tissues received two quick, two five, and two ten-minute washes in 0.1M PBS at physiological pH. Sections were incubated for one hour with donkey anti-rabbit (1:500, IgG conjugated Alexa 488), donkey anti-goat (1:500, IgG conjugated Alexa 594), and donkey anti-mouse (1:200, IgG conjugated Alexa 488) secondary antibodies from Jackson ImmunoResearch Laboratories Inc. Tissues were mounted on to glass slides with Vectashield Antifade Mounting Medium with DAPI (Vector Laboratories) and coverslipped. Care was taken to ensure that each tissue section was sampled from the same relative region of the spinal cord between animals, for a given experiment. A no-primary control was run for all antibodies to reduce the probability of alpha type I and beta type II errors. Quantification was performed in the lateral funiculus surrounding the dorsal horn of the spinal cord, directly contralateral to the spinal lesion (Fig. 4B). This region was chosen to ensure analysis of white matter axons that were anatomically intact, as previously described (Arvanian et al., 2009; Hununyan et al.,

2010). Experimenters were blinded to animal identity and treatment to reduce bias in the quantitative analysis.

Quantification of the node of Ranvier sodium channels and paranodal integrity

Quantification of normal and abnormal node of Ranvier was completed by immunostaining 30-um thick transverse tissue sections (obtained from spinal cord segments T7-T10) for Nav1.6 and caspr antigens. The y-coordinate of the region of interest (ROI) was determined by dividing the manually-measured rostral-caudal lesion cavity diameter in half, to give the radial epicenter of the injury site. The tissue was scanned laterally and a final image with a 1-tile height was acquired in the contralateral white matter. The length of the image varied between tissue sections, and animals, depending on the size of intact white matter in the tissue section. For each image, the entire width of the lateral funiculus was photographed. Images were obtained using a Zeiss Axio Imager Apotome scope with a 40x air objective. A z-stack series was obtained composed of 10 tiled images, each 1-um apart. The 10-um thick portion of each tissue included in the z-stack series was chosen as the most visibly- clear z-region in each tissue section. The 10 consecutive individually-tiled images were stacked using the “Images to Stack” tool in the “Image” menu of ImageJ. The image stack was then subdivided in square sections, using an overlay grid (area per point for each grid square: 5.41 $in.^2$), to avoid duplicate node counting. The “Cell Counter” plugin was used to record node count.

Node counts were binned into three categories: 1) normal node of Ranvier identified by a high-intensity Nav1.6-positive cluster of approximately 1-um in diameter and paranodally

flanked by two (one per side) bright caspr-positive marks, as previously described (Taylor et al., 2017), 2) heminode of Ranvier identified by one flank of bright caspr-positive mark accompanied by the presence or absence of a Nav1.6-positive cluster, and 3) empty node of Ranvier identified by two flanking caspr-positive marks without a bright Nav1.6-positive cluster within the node. The total node count within a given z-stack slice was divided by the total area quantified to obtain a normalized node count per um^2 per animal. This value was multiplied by 100 to yield a percent. A group average was obtained and analyzed using the statistical methods described below.

Quantification of oligodendrocytes and apoptotic cells

Images were obtained using a Zeiss Axio Imager Apotome scope with a 40x air objective. Z-stack images were acquired similarly to that performed in the Nav1.6/caspr quantification, except that a z-stack consisted of four images, 3-um apart, over a 9-um z-height. Oligodendrocyte cell counts were binned into two categories: 1) “oligodendrocyte progenitor” identified by a high-intensity GSTpi nuclear localization mark ($nucGSTpi^+/DAPI^+$) or 2) “pre-oligodendrocyte or older” identified by a cytosolic GSTpi mark ($cytGSTpi^+/DAPI^+$). Apoptotic cells were defined by a high-intensity cleaved caspase-3^+ mark counterstained with DAPI. The total counts of oligodendrocytes and apoptotic cells, in a given z-stack slice, were divided by the total area quantified to obtain normalized values per um^2 per animal. These values were multiplied by 100. A group average was obtained and analyzed using the statistical methods described below.

Quantification of reactive astrocyte process extension

Images were obtained on a Zeiss Axiophot fluorescent microscope using a 20x objective. The optimal exposure and signal-to-noise ratio were determined and held constant across all images and animals. The y-coordinate of the region of interest (ROI) was determined by dividing the manually-measured rostral-caudal lesion cavity diameter in half, to give the radial epicenter of the injury site. The tissue was scanned laterally and one tile of a 20x image was obtained in the lateral funiculus of the spinal cord contralateral to the lesion. Images were taken in approximately the same region across all sections and animals. Using ImageJ, a fluorescent signal threshold was set such that intensities at or above the threshold were qualified as $GFAP^+$ reactive astrocyte processes. Conversely, fluorescent pixels below the determined threshold were treated as background signal. All $DAPI^+$ nuclei were manually quantified within the image and normalized to the area of the image to give a cell density value.

Statistical analysis

One-way ANOVA (with or without interactions) and Pearson correlations were used to determine statistical significance for immunohistochemistry data (Nav1.6/caspr node of Ranvier, oligodendrocytes, apoptosis, astrocytes). A Welch's t-test was used to determine the significance of the injury severity analysis. Two-way ANOVA with Tukey's HSD (Honest Significant Difference) post-hoc test was used to determine the relationships of significance for the behavioral results. Data was assessed for normality using the Shapiro-Wilk normality test and normal quantile-quantile plot. The statistical analysis was performed using R Studio and the significance level was set at $p=0.05$.

Results

Epidural stimulated and step trained rats displayed improved step height of the injured side compared to step training alone

To understand how the effect of chronic ES post-SCI on motor function, we evaluated step height of the leg corresponding to the injured side of the spinal cord (right leg) at day 29 post-injury. Group step height averages were compared between Tr animals and ES+Tr animals in absence (ES+Tr-Off) and presence (ES+Tr-On) of stimulation. This analysis showed statistically significant differences in step height at day 29 post-injury between groups, but not stimulation conditions (Fig. 5B). This indicates that, by 29 days post-injury, chronic ES is associated with persistent motor effects that are apparent in rats for at least 24 hours after the last ES session. Further, it demonstrates the ability for ES+Tr animals to become less dependent on ES for motor functional improvement (ES+Tr-Off vs. ES+Tr-On, Fig 5B). There was no difference in step height deficits or recovery for the uninjured side (left leg), which is consistent with a hemisection injury (5,6). Further efforts will be made to determine ES effects on step drag duration, inter-limb coordination, and how these parameters relate to functional motor recovery with ES post-SCI. There was no statistically significant difference in the lesion cavity area between groups (Fig. 6A). Values are reported as a percentage of the total section area.

Fewer abnormal node of Ranvier were present in epidural stimulated and step trained rats compared to step training alone

To determine the effect of ES on the node of Ranvier in anatomically intact spinal axons, the number of normal and abnormal node of Ranvier (defined in Materials and Methods) was assessed in the contralateral white matter across from the spinal lesion in one tissue per animal (composed of a z-stack of 10 images per tissue) sampled from the dorsal region of the spinal cord (Fig. 4B). We observed a reduction in the proportion of abnormal nodes in this spinal region for animals that received ES, indicating an association between ES and reduced nodal pathology (Fig. 7B). Heminodes composed the majority (≥ 50%) of pathological nodes in both groups, however, there were markedly fewer heminodes in animals that received ES (Fig. 7C). These results indicate a change in total node composition, highlighting the potential physiological importance of heminodes post- SCI and their involvement in ES-facilitated motor recovery. Four animals per group were included in the nodal analysis due to exclusion of two outliers and practical limitations in tissue processing. Future efforts will be made to increase the number of tissues sampled.

The number of apoptotic cells was indirectly correlated with the occurrence of heminodes of Ranvier in epidural stimulated and step trained rats, but not step training alone

Because the node of Ranvier is contacted and modulated by various glial networks for mediation of axonal function, anatomically intact white matter tissue contralateral to the spinal lesion (Fig. 4B) was analyzed to determine a correlation between programmed white matter cell death (via apoptosis) and abnormal node of Ranvier. We demonstrated

that epidural stimulation is associated with a stronger correlation between apoptotic cells and heminodal pathology, compared to Tr animals (Fig. 8). These data demonstrate that an increase in the number of heminodes is correlated with decreasing apoptotic white matter when ES it utilized, marking the potential importance of white matter glial cells and nodal integrity in the ES model. There is a weak and statistically nonsignificant correlation between apoptotic cells and heminodes of Ranvier in Tr animals. There was no difference in the number of apoptotic oligodendrocytes between groups. Together, these data may suggest that ES mediates glial cells and the node of Ranvier for improved motor function. Efforts will be made to increase samples sizes to increase statistical confidence in this result.

Increased oligodendrocyte progenitors, but not cell density, was associated with epidural stimulation and step training compared to step training alone

Given the association between apoptotic white matter cells and axonal integrity, as measured by the number of abnormal node of Ranvier in anatomically intact white matter axons, an effort was made to determine the effect of ES on glial cells in this region. We demonstrated that epidural stimulation was associated with a statistically significant increase in the number of oligodendrocyte progenitors ($nucGSTpi^+/DAPI^+$), but no difference in the number of pre-oligodendrocytes and older ($cytGSTpi^+/DAPI^+$) (Fig. 9A). There was no difference in cell density (total $DAPI^+$ count per 500um x 500um x 9um region) between groups, indicating that a change in total cell composition may be important in ES-facilitated motor recovery (Fig. 9B).

Epidural stimulation is associated with a stronger and less variable correlation between reactive fibrous astrocyte processes area and oligodendrocyte progenitors

Given the well-established inter-glial communication and modulation of axonal function by glial networks, we investigated the effect of ES on astrocytes, as measured by the area of reactive fibrous astrocytic process extension, in the anatomically intact white matter of the spinal cord contralateral to the lesion. It was important to investigate astrocytes because, not only are they the most numerous cell type in the CNS, but they also show a reaction to injury. Although there was no statistical difference in the astrocytic process area between groups (Fig. 10A), ES+Tr animals showed a stronger and statistically significant positive correlation between astrocyte process extension area and oligodendrocyte progenitors (Fig. 10B). While the slopes were relatively similar (Fig. 10B), ES+Tr animals displayed significantly lower variability in the correlation, indicating possible modulation of astrocyte efficiency and how this relates to oligodendrocyte progenitor differentiation, proliferation, and/or function. This idea is supported by the finding that overall cell count ($DAPI^+$ cells) was not different between groups. The GFAP-oligodendrocyte progenitor data were derived from different tissues and cell counts from those presented in Fig. 9A, due to host reactivity limitations that affected the number of different antibodies used to saturate each tissue section. Overall, these data were composed of 9 and 11 dorsal tissue sections from the ES+Tr and Tr groups respectively, across 6 different animals per group.

Discussion

The purpose of this study was to determine associated pathways involved in ES-mediated motor recovery. This is the first study to demonstrate that chronic use of ES (more than 20 sessions of 35-minute duration) post- lateral hemisection in rats provides functional motor improvement that persists for at least 24 hours after the last stimulation session. Further, we demonstrated that ES is associated with the following neuroplastic changes in spinal white matter that survives the initial injury: 1) reduced node of Ranvier pathology, 2) increase in oligodendrocyte progenitor populations, and 3) strengthened correlation between reactive fibrous astrocytic processes and oligodendrocyte progenitors. These novel findings are the first evidence of cellular neural plasticity associated with ES-mediated recovery. They demonstrate the potential importance of intact spinal axons and associated glial cells on motor recovery with ES.

Our behavioral results indicated that the use of subthreshold, chronic ES post-SCI improves motor function that persists in the absence of stimulation for at least 24 hours. Further, we demonstrated that there was not a significant difference in step height recovery, in the presence or absence of stimulation, by day 29 if an animal received chronic ES post-SCI. This persistent effect of ES did not become apparent until day 29 post-injury. Together, these data indicate that the consistent use of ES post-injury can modulate neural circuitry to a critical degree that allows the neural system to become independent of ES for facilitation of motor function. It leads us to consider whether chronic ES use may help an individual regain autonomous motor function such that they become less dependent on ES over time- A favorable outcome for the SCI population.

The finding that ES+Tr animals performed similarly by day 29 post-SCI, regardless of ES on or off, indicates significant neuroplasticity associated with ES-mediated recovery. Understanding the cellular mechanisms underlying this process is critical to optimizing the implementation of ES as a prescribed treatment for motor dysfunction post-SCI. Previous studies reported that post-SCI, presumably anatomically intact axons in the contralateral white matter, that survive the initial injury, display pathological features such as dispersed sodium channels and nodal decomposition associated with motor dysfunction (Arvanian et al., 2009; Hununyan et al., 2010). The present observations demonstrate a lower incidence of the node of Ranvier pathology in rats that received ES with step training compared to step training alone. The combination of these results is consistent with the idea that Nav1.6 clusters at the node of Ranvier could be a critical feature of the demonstrated motor recovery.

We also demonstrated that ES+Tr animals displayed a strong correlation between the heminodes of Ranvier and apoptotic cells in the surrounding white matter. Tr animals showed a slight negative correlation that did not reach statistical significance. These data may suggest that apoptosis has a functional advantage when ES is utilized post-SCI. It is possible that cells detrimental to nodal and axonal integrity undergo programmed cell death when ES and step training are combined as post-SCI therapy. Resident and infiltrating immune cells may have a detrimental effect on axonal function after CNS injury by engulfing myelin surrounding axons and contributing to axonal degradation (Kopper

and Gensel, 2017). These data are consistent with potential ES-mediated facilitation of the post-SCI inflammatory response and perhaps contribute to motor improvement.

We observed an increase in the number of oligodendrocyte progenitors in rats that received ES with step training compared to step training alone. To understand the functional implications of this increase, we determined their correlation with the area of reactive fibrous astrocytic processes. This was important because astrocytes exhibit waves of calcium coordinated with electrical stimulation (Clarke et al., 2017; Gibson et al., 2014). Further, they exert control over the proliferation and differentiation of oligodendrocyte progenitors (Halassa et al., 2007; Nedergaard et al., 2003; Sofroniew et al., 2009). In addition, astrocytes contact the node of Ranvier and affect axonal integrity during both nonpathological and pathological states (Halassa et al., 2007; Nedergaard et al., 2003; Sofroniew et al., 2009). The current study demonstrated a clear relationship between the area of astrocytic processes and the number of oligodendrocyte progenitors in both the Tr and ES+Tr groups. The interesting observation relative to this relationship, however, was a markedly reduced variation in this correlation in ES+Tr animals. With the addition of ES, the correlation changed from $r=0.52$ ($p=0.10$) to $r=0.81$ ($p=0.008$). Theoretically, this change could be interpreted to indicate that astrocytes exerted a tighter control over the generation of oligodendrocyte progenitors, but also the reverse. Additionally, it is possible that astrocytes play a role in transferring the electrical stimulus from the stimulation site at the lumbosacral spinal cord to the thoracic spinal cord where we demonstrated neuroplastic histological changes. These results indicate that the

oligodendrocyte progenitor- astrocyte relationship, and how it relates to motor function and myelination, needs to be examined more thoroughly in subsequent studies.

These data demonstrate that the combination of chronic ES and step training is not only associated with greater improvement in locomotor function compared to step training only, but also indicates the potential importance of both surviving axon node of Ranvier and associated glial cells. The improved motor function was linked to a reduced level of pathology associated with the node of Ranvier, an increased number of oligodendrocyte progenitors, and a strengthened correlation between these cells and reactive astrocytic process area. It is important to consider the fact that there were multiple cellular changes associated with the demonstrated improvement in motor function, and perhaps more importantly, these changes in cellular properties were observed in spinal tissues contralateral to the site of the induced lesion. This implies that the functional deficits apparent post-SCI are not likely attributable only to the tissues that are presumably initially disrupted and highlights the idea that presumably intact fibers can be potential therapeutic targets of ES post-SCI. Further research should be done to determine the direct association between the electrophysiological properties of these axons and the pathology identified in the spinal tissues.

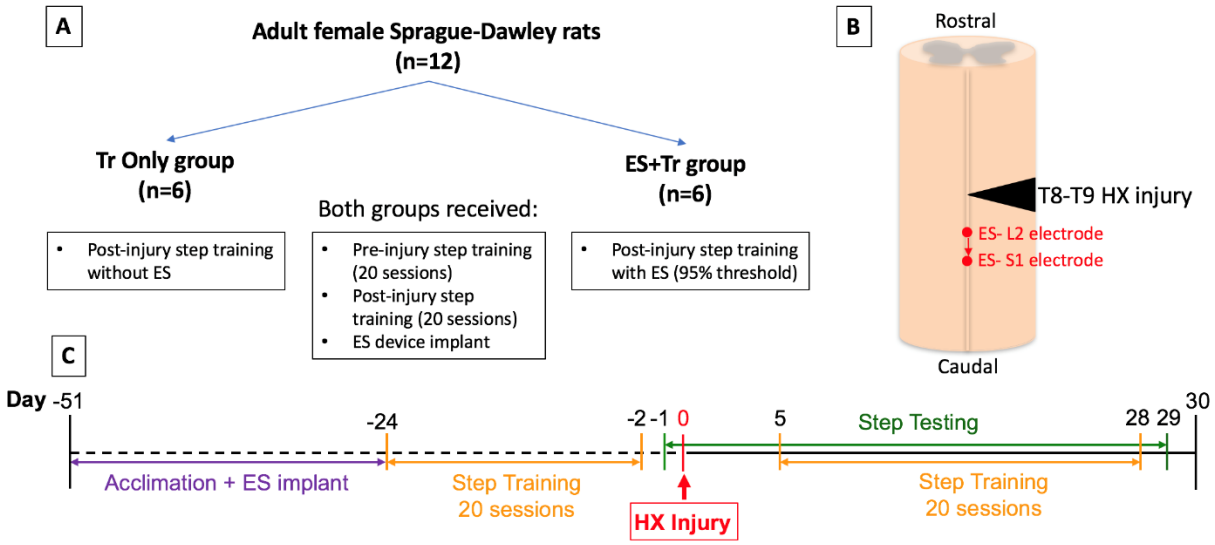

Figure 1. Experimental design and timeline. (A) Experimental design schematic demonstrating that adult female Sprague-Dawley rats (n=12) were divided into cohorts such that half received either post-injury step training alone (Tr, n=6) or step training with ES (ES+Tr, n=6). Both groups received pre- and post-injury step training and a epidural stimulation implant. **(B)** Injury and ES stimulation schematic demonstrating the relative location of right lateral hemisection injury and distal ES implant. **(C)** Rats were implanted with an epidural stimulator and underwent pre-injury step training for 20 sessions. Animals were step tested one day before surgery and allowed 4 full days of recovery. Animals then underwent post-injury step training (35 min/ session) for 20 sessions over 28 days, given a rest day, and step tested before sacrifice at day 30.

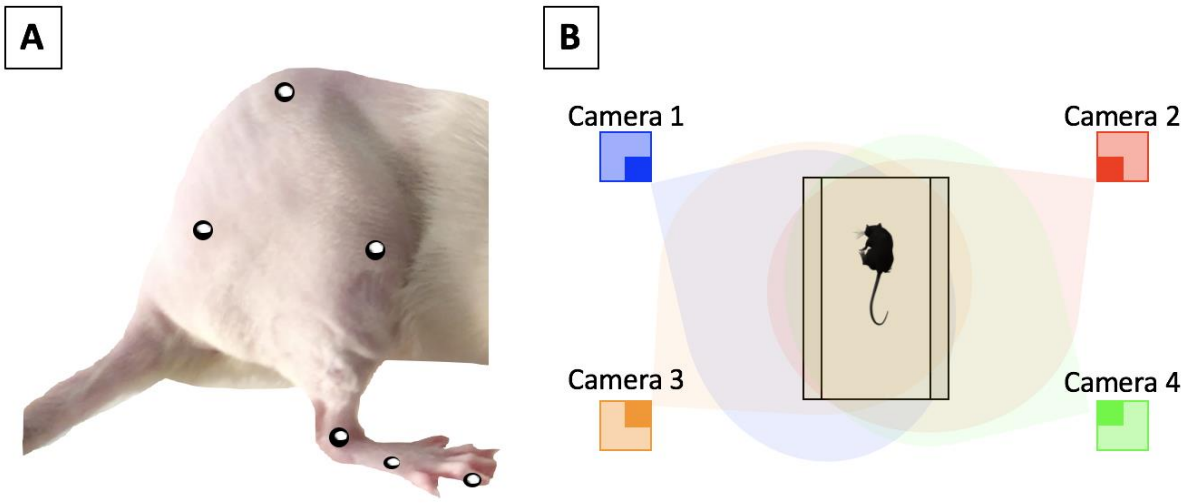

Figure 2. Locomotor testing marker placement and step testing set-up. (A) Prior to locomotor testing, retroreflective markers were placed on the skin directly overlaying the anterior superior iliac spine of the iliac crest, greater trochanter of the femur, lateral condyle of the tibia, lateral malleolus of the tibia, the distal end of the fifth metatarsal, and the lateral surface of the fourth metatarsal. Markers aided in visualization of these joints as the animal moved in space. **(B)** The rat was positioned on the treadmill and surrounded by four cameras that captured a three-dimensional coordinates of the joint location in space during locomotion.

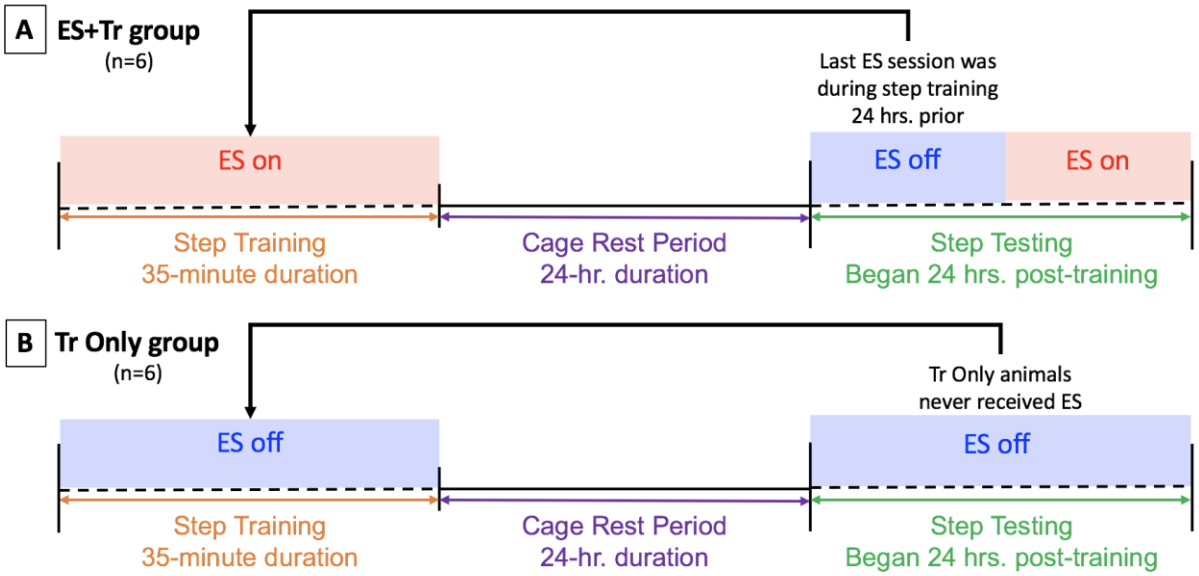

Figure 3. Locomotor training and testing schematic for ES+Tr and Tr rats. All animals were step tested 24 hours after their last step training session. All step testing sessions were composed of approximately 10 consecutive steps per condition. **(A)** ES+Tr stepping ability was always captured under the ES off condition before ES on. This design allowed for the assessment of inherent stepping ability prior to acute facilitation provided by ES. **(B)** Tr animals never received ES- Step training and testing were conducted without ES, despite the implant present.

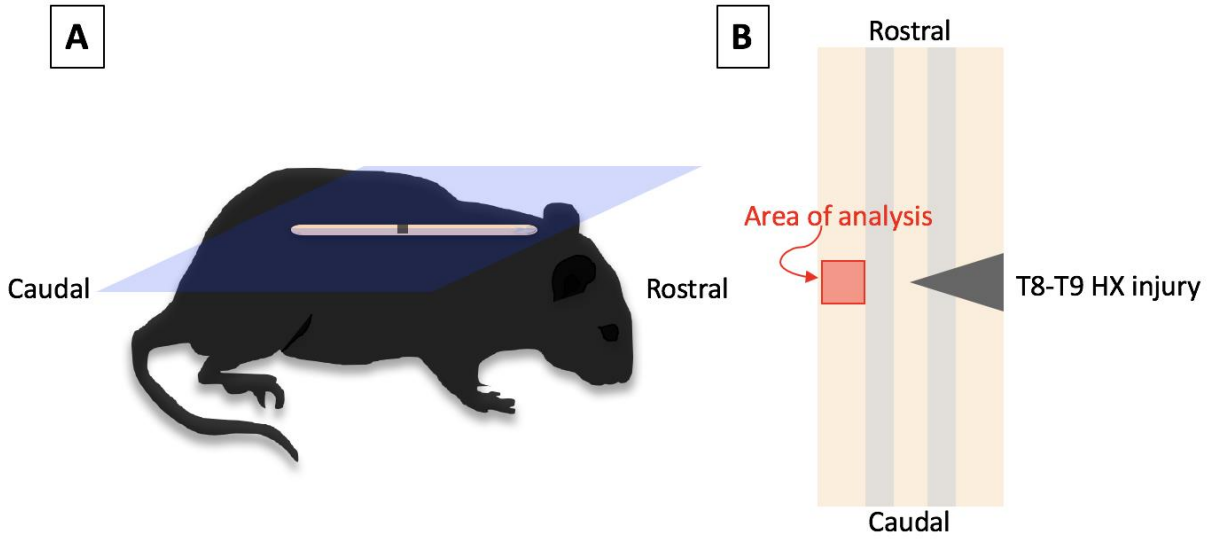

Figure 4. Tissue sampling schematic and region of histological analysis. (A) Transverse spinal cord tissue sections were obtained in the dimension indicated by the (blue) plane. **(B)** Analysis of the node of Ranvier, oligodendrocytes, astrocytic processes, and cell apoptosis was performed in the white matter contralateral to the spinal lesion (red).

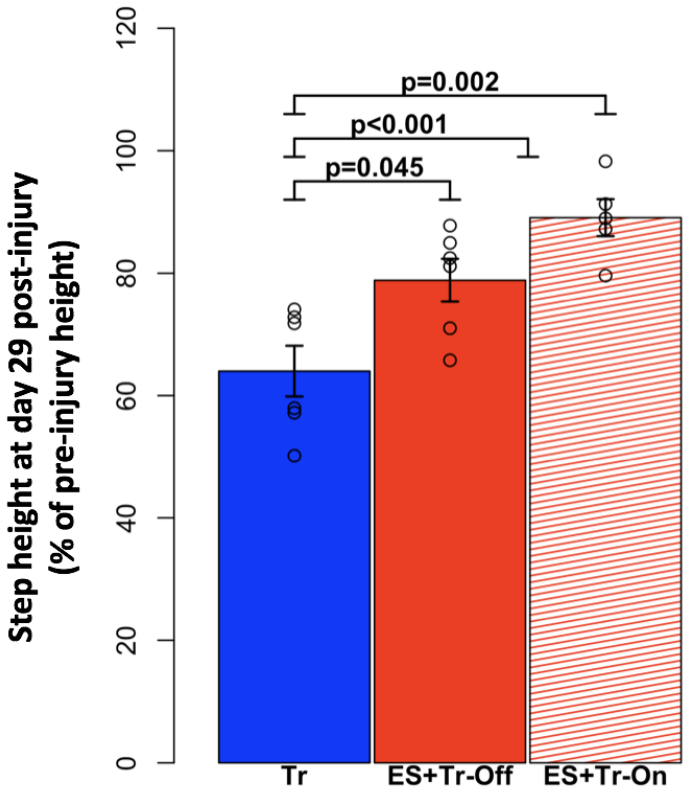

Figure 5. Epidural stimulation is associated with improved step height recovery of the injured side at day 29 post-injury. ES+ Tr animals displayed improved step height by day 29 post-injury compared to Tr animals in the presence of ES (89.07% ± 3.02% ES+Tr-On; 63.99% ± 4.14% Tr) and absence for at least 24 hours (78.85% ± 3.51% ES+Tr-Off). This demonstrated the ability for ES to modulate behavior after stimulation had ceased. Tr animals stepped significantly lower than ES+Tr animals regardless of ES off or on (83.50% ± 2.76% ES+Tr, n=11). There was no statistical difference in step height between ES off and on conditions by day 29, indicating that ES+Tr animals had become relatively independent of the stimulation with chronic ES treatment post-SCI.

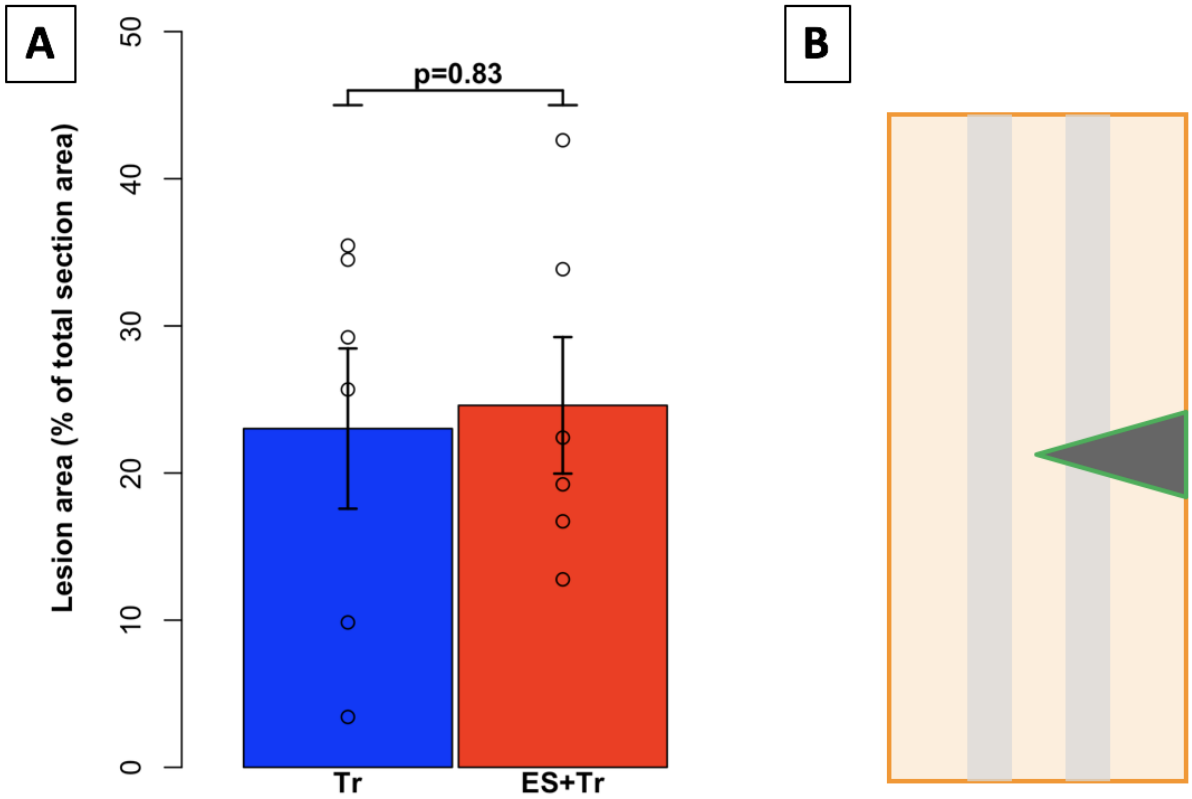

Figure 6. No statistical difference in lesion cavity area between ES+Tr and Tr rats. (A) Tissue analysis at 30 days post-injury revealed no difference in the cystic cavity lesion area between groups (23.02% ± 5.45% Tr; 24.60% ± 4.64% ES+Tr, n=6). **(B)** Cavities were manually outlined in ImageJ, as demonstrated (green), to obtain a cavity area (um^2) that was then divided by the total tissue area of the section (orange) and multiplied by 100 to obtain a lesion area percent.

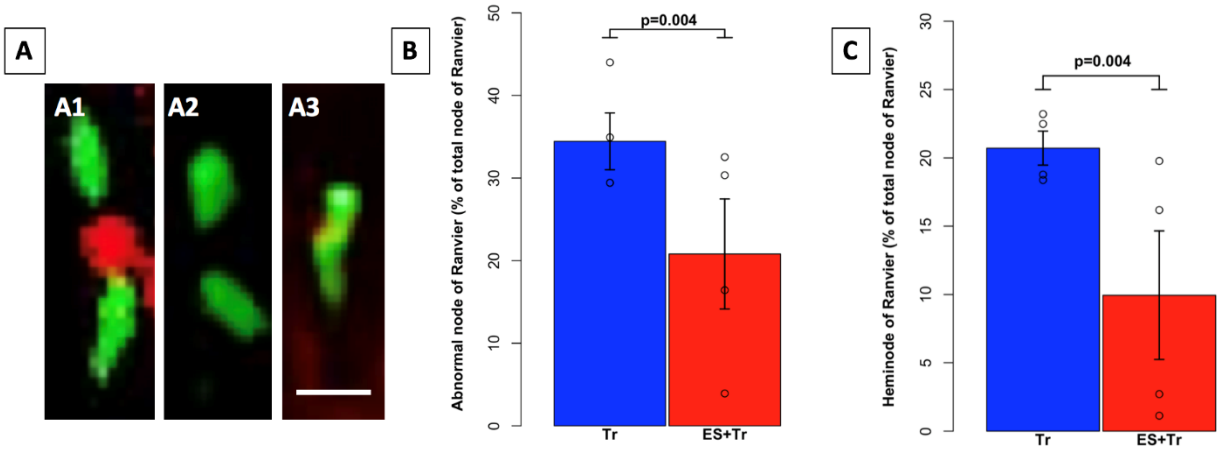

Figure 7. ES with step training is associated with reduced node of Ranvier pathology in anatomically intact spinal axons. (A) Depiction of normal **(A1)** and abnormal **(A2-A3)** node of Ranvier as demonstrated by paranodal caspr (green) and nodal Nav1.6 (red). A2 and A3 indicate an empty and heminode of Ranvier, respectively, which are hallmarks of neurodegenerative- neuropathological states. **(B)** Values were calculated according to 100*(A2+A3/ sum(A1:A3)). ES+Tr animals displayed reduced nodal pathology, as evidenced by a reduction in the proportion of abnormal (empty + hemi) node of Ranvier (20.81% ± 6.66% ES+Tr, n=4), compared to Tr animals (34.45% ± 3.44% Tr, n=4) with $p<0.01$. **(C)** Values were calculated according to 100*(A3/ sum(A1:A3)). ES+Tr animals displayed a lower proportion of the nodal population that are heminodes of Ranvier (9.95% ± 4.70% ES+Tr, n=4) compared to Tr animals (20.72% ± 1.24% Tr, n=4) with $p<0.01$. Scale bar= 1 um.

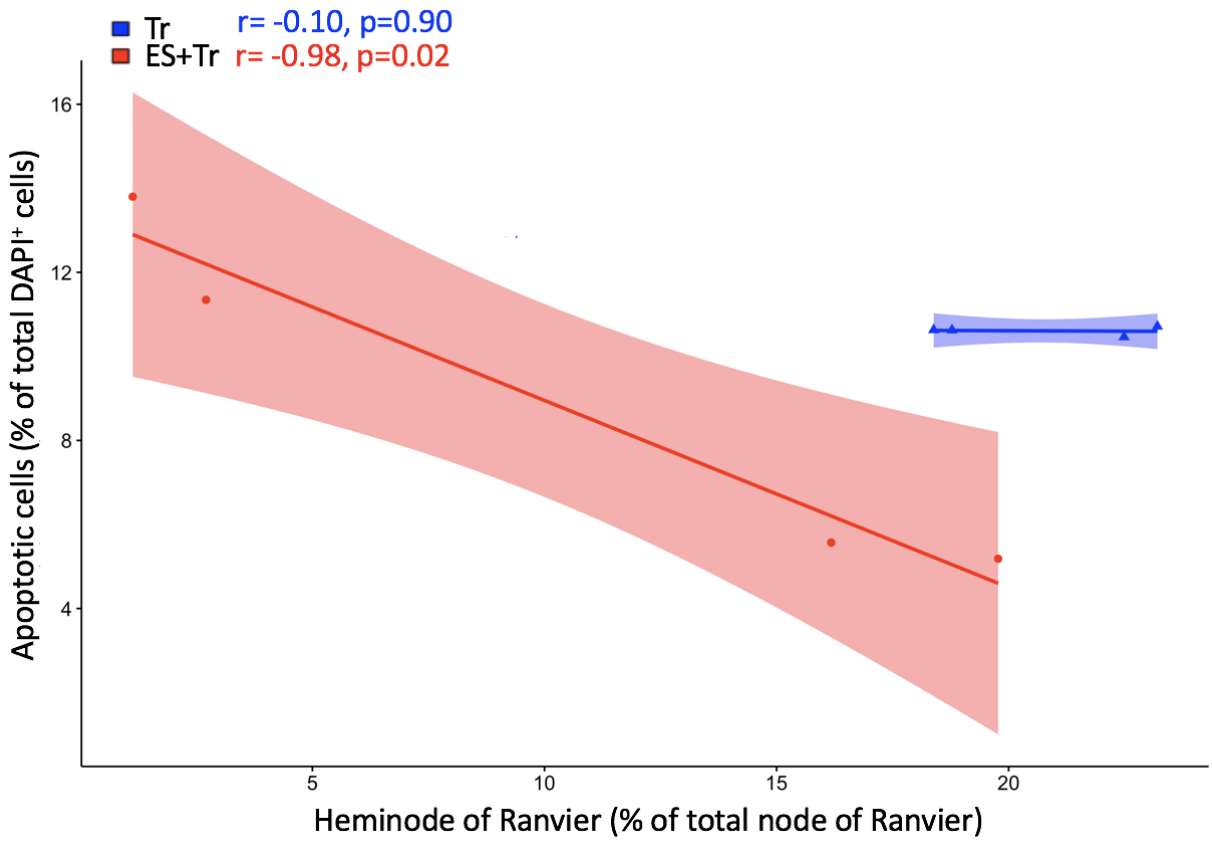

Figure 8. Indirect correlation between apoptosis and heminodes in ES+Tr rats. ES+Tr animals (r= -0.98, p=0.02 ES+Tr, n=4) compared to Tr animals (r= -0.10, p=0.90 Tr, n=4) demonstrate that ES is associated with an altered Pearson correlation between cell death and nodal pathology in contralateral white matter post-SCI.

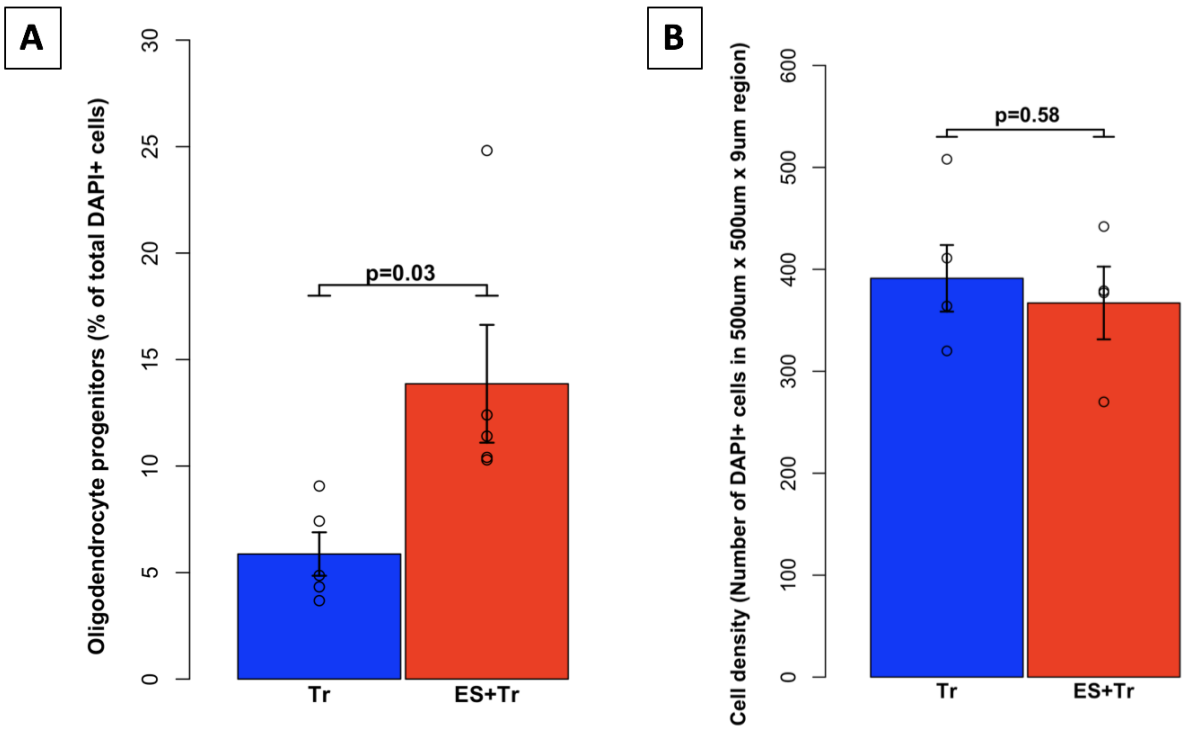

Figure 9. Increased oligodendrocyte progenitors, but not cell density, in ES+Tr rats. (A) Animals that received ES displayed a higher percentage of total cells in the white matter ($DAPI^+$) that were oligodendrocyte progenitors (13.86% ± 2.77% ES+Tr, n=5) compared to animals that received step training only (5.87% ± 1.02% Tr, n=5). **(B)** No statistically significant difference between groups for cell density ($DAPI^+$ cell count per 500um x 500um x 9um region) in the contralateral white matter across from the spinal lesion.

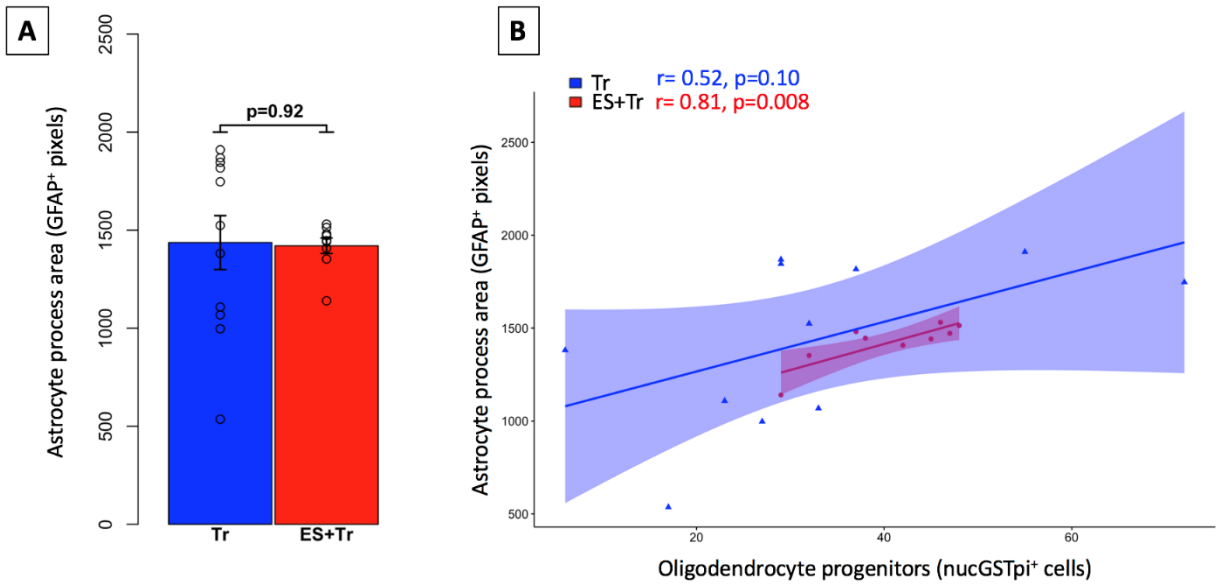

Figure 10. ES+Tr animals demonstrate a stronger and less variable relationship between astrocytic processes and oligodendrocyte progenitors. (A) No group difference in the number of GFAP$^+$ pixels in the contralateral white matter that survives the initial SCI (1420.78 ± 39.40 GFAP+ pixels ES+Tr, n=6 ; 1436.64 ± 137.47 GFAP+ pixels Tr, n=6) with p>0.05 . **(B)** ES is associated with a subtle, yet stronger, correlation between oligodendrocyte progenitors and astrocyte process extension such that this relationship becomes statistically significant in ES+Tr animals. Further, there is a marked reduction of the variation in the predictability of this relationship, indicating the potential impact of ES on inter-glial functional efficiency.

References

1. Angeli CA, Edgerton VR, Gerasimenko YP, Harkema SJ. Altering spinal cord excitability enables voluntary movements after chronic complete paralysis in humans. Brain. 2014;137:1394-409.

2. Arvanian VL, Schnell L, Lou L, Golshani R, Hunanyan A, Ghosh A, Pearse DD, Robinson JK, Schwab ME, Fawcett JW, Mendell LM. Chronic spinal hemisection in rats induces a progressive decline in transmission in uninjured fibers to motoneurons. Exp Neurol. 2009;216(2):471-80.

3. Charles AC, Merrill JE, Dirksen ER, Sanderson MJ. Intercellular signaling in glial cells: calcium waves and oscillations in response to mechanical stimulation and glutamate. Neuron. 1991;6(6):983-92.

4. Clarke D, Penrose MA, Penstone T, Fuller-Carter PI, Hool LC, Harvey AR, Rodger J, Bates KA. Frequency-specific effects of repetitive magnetic stimulation on primary astrocyte cultures. Restor Neurol Neurosci. 2017;35(6):557-569.

5. Craig A, Tran Y, Middleton J. Psychological morbidity and spinal cord injury: a systematic review. Spinal Cord. 2009;47(2):108-14.

6. Domingues HS, Portugal CC, Socodato R, Relvas JB. Oligodendrocyte, astrocyte, and microglia crosstalk in myelin development, damage, and repair. Front Cell Dev Biol. 2016;4:71.

7. Freeman SA, Desmazières A, Simonnet J, Gatta M, Pfeiffer F, Aigrot MS, Rappeneau Q, Guerreiro S, Michel PP, Yanagawa Y, Barbin G, Brophy PJ, Fricker D, Lubetzki C, Sol-Foulon N.Proc Natl Acad Sci U S A. Acceleration of conduction velocity linked to clustering of nodal components precedes myelination. 2015;112(3):E321-8.

8. Gerasimenko YP, Lu DC, Modaber M, Zdunowski S, Gad P, Sayenko DG, Morikawa E, Haakana P, Ferguson AR, Roy RR, Edgerton VR. Noninvasive Reactivation of Motor Descending Control after Paralysis. J Neurotrauma. 2015;32(24):1968-80.

9. Gibson EM, Purger D, Mount CW, Goldstein AK, Lin GL, Wood LS, Inema I, Miller SE, Bieri G, Zuchero JB, Barres BA, Woo PJ, Vogel H, Monje M.Science. Neuronal activity promotes oligodendrogenesis and adaptive myelination in the mammalian brain. 2014;344(6183):1252304.

10. Halassa MM, Fellin T, Takano H, Dong JH, Haydon PG. Synaptic islands defined by the territory of a single astrocyte. J Neurosci. 2007;27(24):6473-7.

11. Harkema H, Gerasimenko Y, Hodes J, Burdick J, Angeli C, Chen Y, Ferreira C, Willhite A, Rejc E, Grossman RG, Edgerton VR. Effect of epidural stimulation of

the lumbosacral spinal cord on voluntary movement, standing, and assisted stepping after motor complete paraplegia: a case study. Lancet. 2011;377(9781):1938-47.

12. Henry MA, Freking AR, Johnson LR, Levinson SR. Sodium channel Nav1.6 accumulates at the site of infraorbital nerve injury. BMC Neurosci. 2007;8: 56.

13. Hunanyan AS, Alessi V, Patel S, Pearse DD, Matthews G, Arvanian VL. Alterations of action potentials and the localization of Nav1.6 sodium channels in spared axons after hemisection injury of the spinal cord in adult rats. J Neurophysiol. 2011;105(3):1033-44.

14. Huxley AF, Stämpfli R. Evidence for saltatory conduction in peripheral myelinated nerve fibres. J Physiol. 1949;108(3):315-39.

15. Kopper TJ, Gensel JC. Myelin as an inflammatory mediator: Myelin interactions with complement, macrophages, and microglia in spinal cord injury. J Neurosci Res. 2017. [Epub ahead of print]

16. Leferink PS, Heine VM. The healthy and diseased microenvironments regulate oligodendrocyte properties: Implications for regenerative medicine. Am J Pathol. 2017. [Epub ahead of print]

17. Liebscher T, Schnell L, Schnell D, Scholl J, Schneider R, Gullo M, Fouad K, Mir A, Rausch M, Kindler D, Hamers FP, Schwab ME. Nogo-A antibody improves regeneration and locomotion of spinal cord-injured rats. Ann Neurol. 2005;58(5):706-19.

18. National Research Council. Guide for the care and use of laboratory animals, Eighth Edition Edition. Washington, DC: National Academy Press; 2011.

19. Nedergaard M, Ransom B, Goldman SA. New roles for astrocytes: redefining the functional architecture of the brain. Trends Neurosci. 2003;26(10):523-30.

20. Pêgo AP, Kubinova A, Cizkova D, Vanicky I, Mar FM, Sousa MM, Sykova E. Regenerative medicine for the treatment of spinal cord injury: more than just promises? J Cell Mol Med. 2012; 16(11): 2564–2582.

21. Roy RR, Hutchison DL, Pierotti DJ, Hodgson JA, Edgerton VR. EMG patterns of rat ankle extensors and flexors during treadmill locomotion and swimming. J Appl Physiol. 1991;70:2522–9.

22. Shah PK, Gerasimenko Y, Shyu A, Lavrov I, Zhong H, Roy RR, et al. Variability in step training enhances locomotor recovery after a spinal cord injury. Eur J Neurosci. 2012;36:2054–62.

23. Sofroniew MS, Vinters HV. Astrocytes: biology and pathology. Acta Neuropathol. 2010; 119(1): 7–35.

24. Susuki K, Chang KJ, Zollinger DR, Liu Y, Ogawa Y, Eshed-Eisenbach Y, Dours-Zimmermann MT, Oses-Prieto JA, Burlingame AL, Seidenbecher CI, Zimmermann DR, Oohashi T, Peles E, Rasband MN. Three mechanisms assemble central nervous system nodes of Ranvier. Neuron. 2013;78(3):469-82.

25. Taylor AM, Saifetiarova J, Bhat MA. Postnatal loss of neuronal and glial neurofascins differentially affects node of Ranvier maintenance and myelinated axon function. Front Cell Neurosci. 2017;11:11.

26. Wang HF, Liu XK, Li R, Zhang P, Chu Z, Wang CL, Liu HR, Qi J, Lv GY, Wang GY, Liu B, Li Y, Wang YY. Effect of glial cells on remyelination after spinal cord injury. Neural Regen Res. 2017;12(10):1724-1732.

27. Waxman SG, Black JA, Sontheimer H, Kocsis JD. Glial cells and axo-glial interactions: implications for demyelinating disorders. Clin Neurosci. 1994;2(3-4):202-10.